

Fatigue failure of amorphous alloys under cyclic shear deformation

Nikolai V. Priezjev^{1,2}

¹*Department of Civil and Environmental Engineering,
Howard University, Washington, D.C. 20059 and*

²*Department of Mechanical and Materials Engineering,
Wright State University, Dayton, OH 45435*

(Dated: January 20, 2023)

Abstract

The accumulation of plastic deformation and flow localization in amorphous alloys under periodic shear are investigated using molecular dynamics simulations. We study a well-annealed binary mixture of one million atoms subjected to oscillatory shear deformation with strain amplitudes slightly above a critical value. We find that upon approaching a critical strain amplitude from above, the number of shear cycles until the yielding transition is well described by a power-law function. Remarkably, the potential energy at the end of each cycle as a function of the normalized number of cycles is nearly independent of the strain amplitude, which allows for estimation of the fatigue lifetime at a given strain amplitude. The analysis on nonaffine displacements of atoms elucidates the process of strain localization, including irreversible rearrangements of small clusters until the formation of a system-spanning shear band.

Keywords: metallic glasses, fatigue, yielding transition, cyclic loading, molecular dynamics simulations

I. INTRODUCTION

The prediction of stability and lifetime of amorphous alloys under repeated stress or strain deformation is important for various structural applications [1, 2]. Although multicomponent alloys like metallic glasses possess a number of advantageous properties, such as high strength and large elastic strain limit, their resistance to fatigue damage is relatively poor [3–6]. The failure mechanism in metallic glasses involves the formation of nanoscale shear bands where plastic strain becomes strongly localized, which in turn might lead to propagation of microscale cracks [7–10]. At the atomic level, the elementary plastic deformation in amorphous solids consists of rapid rearrangement of a small cluster of particles or shear transformation [11, 12]. Notably, the results of numerical simulations of the fibre bundle model have shown that the fatigue failure under repeated loading of heterogeneous materials occurs after a number of cycles, and the fatigue lifetime has a power-law dependence on the loading amplitude [13]. More recently, using two models of elastoplastic rheology, it was demonstrated that cyclically sheared amorphous materials initially accumulate low levels of damage in the form of spatial strain heterogeneity, which is followed by a sudden catastrophic material failure via shear band formation [14]. However, in spite of the considerable modeling and experimental efforts, the precise determination of the critical loading amplitude and fatigue lifetime remains a challenging problem.

During the last decade, the effect of cyclic loading on the yielding transition, structural relaxation, and flow localization in amorphous materials was extensively studied using atomistic simulations [15–40]. Interestingly, it was demonstrated that in the athermal limit, amorphous solids under small-amplitude oscillatory shear evolve into the so-called limit cycles, where trajectories of atoms become exactly reversible after one or more periods, and the number of cycles to reach periodic behavior diverges upon approaching a critical strain amplitude from below [18, 41]. On the other hand, periodic deformation at strain amplitudes above a critical value leads to yielding and flow localization after a number of cycles [19, 23, 24, 27, 31]. In general, the number of cycles until the yielding transition depends on the degree of annealing, temperature, system size, strain amplitude and frequency. In particular, it was found that the number of cycles to failure increases upon increasing frequency [19] or glass stability [29, 32], and by decreasing strain amplitude towards a critical value [19, 24]. In addition, the number of fatigue cycles can be reduced by periodically

alternating shear orientation in two or three spatial dimensions [31] or by occasionally increasing strain amplitude above a critical value [34]. Despite recent progress, however, the processes of damage accumulation and formation of shear bands during cyclic loading near a critical strain amplitude remain not fully understood.

In this paper, the influence of repeated shear strain on plastic deformation and yielding transition in a disordered solid is studied via molecular dynamics (MD) simulations. We consider a well-annealed binary glass subjected to oscillatory shear deformation at strain amplitudes slightly above a critical value. It will be shown that the number of shear cycles to reach the yielding transition increases approximately as a power-law function when the strain amplitude approaches the critical value. Moreover, we find that the potential energy at zero strain for different strain amplitudes is well described by a single function of the normalized number of cycles. In turn, the appearance of local plastic events and the formation of a shear band at the yielding transition are quantified via the fraction of atoms with large nonaffine displacements during one shear cycle.

The rest of this paper is organized as follows. The details of molecular dynamics simulations as well as the oscillatory shear deformation protocol are described in the next section. The analysis of shear stress, potential energy, and nonaffine displacements is presented in section III. A brief summary is provided in the last section.

II. MOLECULAR DYNAMICS SIMULATIONS

In this study, the amorphous alloy was modeled via the standard Kob-Andersen (KA) binary mixture composed of 80 % of atoms of type A and 20 % of type B [42]. The total number of atoms is 10^6 . In this model, the interaction between atoms of types $\alpha, \beta = A, B$ is defined via the Lennard-Jones (LJ) potential:

$$V_{\alpha\beta}(r) = 4\varepsilon_{\alpha\beta} \left[\left(\frac{\sigma_{\alpha\beta}}{r} \right)^{12} - \left(\frac{\sigma_{\alpha\beta}}{r} \right)^6 \right], \quad (1)$$

where the parameters are set to $\varepsilon_{AA} = 1.0$, $\varepsilon_{AB} = 1.5$, $\varepsilon_{BB} = 0.5$, $\sigma_{AA} = 1.0$, $\sigma_{AB} = 0.8$, $\sigma_{BB} = 0.88$, and $m_A = m_B$ [42]. A similar parametrization was used by Weber and Stillinger to study structure and dynamics of the amorphous metal-metalloid alloy $\text{Ni}_{80}\text{P}_{20}$ [43]. All physical quantities are reported in the units of length, mass, energy, and time, as follows: $\sigma = \sigma_{AA}$, $m = m_A$, $\varepsilon = \varepsilon_{AA}$, and $\tau = \sigma\sqrt{m/\varepsilon}$. The MD simulations were carried out using

the LAMMPS parallel code with the integration time step $\Delta t_{MD} = 0.005 \tau$ and the cutoff radius $r_c = 2.5 \sigma$ [44, 45].

The sample preparation procedure and the deformation protocol are similar to the ones reported in the previous MD study [29]. More specifically, the binary mixture was first placed in a cubic box of linear size $L = 94.10 \sigma$ and equilibrated at the temperature $T_{LJ} = 1.0 \varepsilon/k_B$ and density $\rho = \rho_A + \rho_B = 1.2 \sigma^{-3}$ using the Nosé-Hoover thermostat and periodic boundary conditions [44, 45]. For reference, the critical temperature of the KA model at the density $\rho = 1.2 \sigma^{-3}$ is $T_g = 0.435 \varepsilon/k_B$ [42]. Then, the sample was cooled with computationally slow rate of $10^{-5} \varepsilon/k_B \tau$ from $T_{LJ} = 1.0 \varepsilon/k_B$ to $0.01 \varepsilon/k_B$ at constant density $\rho = 1.2 \sigma^{-3}$. Right after cooling, the glass was subjected to oscillatory shear deformation along the xz plane, as follows:

$$\gamma_{xz}(t) = \gamma_0 \sin(2\pi t/T), \quad (2)$$

where γ_0 is the strain amplitude and $T = 5000 \tau$ is the oscillation period. The simulations were performed for strain amplitudes $0.069 \leq \gamma_0 \leq 0.075$ at $T_{LJ} = 0.01 \varepsilon/k_B$ and $\rho = 1.2 \sigma^{-3}$. The results for the potential energy, shear stress, and nonaffine displacements of atoms are reported only for one realization of disorder because of the considerable computational burden. As an example, it took about 36 days to simulate 800 shear cycles at the strain amplitude $\gamma_0 = 0.069$ using 400 processors in parallel.

III. RESULTS

Recent studies have shown that model glasses prepared by thermal annealing can yield after a certain number of cycles at strain amplitudes that are smaller than the yielding strain during uniform shear deformation [23, 29]. The precise value of the critical strain amplitude is difficult to determine numerically due to a large number of cycles needed to reach the yielding transition. Within the range of about three thousand cycles, it was found that rapidly quenched binary glasses under cyclic loading yield at the critical strain amplitude $\gamma_0 = 0.067$, regardless of whether shear is applied along a single plane or periodically alternated in two or three spatial dimensions [31]. In the present study, we consider a relatively large system of one million atoms and subject a well-annealed KA glass to oscillatory shear deformation at strain amplitudes slightly above the critical value.

We first report the variation of shear stress along the xz plane as a function of time in Fig. 1 for two values of the strain amplitude, i.e., $\gamma_0 = 0.072$ and 0.075 . It can be seen that in both cases, the amplitude of shear stress oscillations slightly decreases upon continued loading until a sudden drop during one shear cycle. Notice that the number of cycles until yielding becomes greater upon decreasing strain amplitude. Specifically, the yielding transition occurs during 218-th cycle for $\gamma_0 = 0.072$ and during 56-th cycle for $\gamma_0 = 0.075$. By contrast, after the yielding transition, the maximum shear stress is determined by the plastic flow within a shear band. These results are consistent with those previously reported for a well-annealed binary glass that was periodically deformed for only 40 shear cycles at larger strain amplitudes [24].

Along with shear stress, we plot in Fig. 2 the time dependence of the potential energy for the same strain amplitudes, $\gamma_0 = 0.072$ and 0.075 , as in Fig. 1. It is evident that the yielding transition is associated with an abrupt increase of the potential energy due to the formation of a shear band across the system. It should be emphasized that for each strain amplitude, the sudden change in shear stress and potential energy occur at the same cycle number. One can further realize that before yielding, the cyclic shear deformation results in a slow accumulation of plastic events. This is reflected in a gradual increase of the potential energy minima when strain is zero as a function of the cycle number.

Next, the potential energy minima at the end of each cycle are presented in Fig. 3 for strain amplitudes in the range $0.069 \leq \gamma_0 \leq 0.075$. Note that the data at zero strain for $\gamma_0 = 0.072$ and 0.075 are the same as in Fig. 2. It can be clearly observed in Fig. 3 that upon reducing strain amplitude towards a critical value, the yielding transition becomes significantly delayed. The exception to this trend is the case of loading at the strain amplitude $\gamma_0 = 0.071$, where the number of cycles until yielding is smaller than for $\gamma_0 = 0.072$. In turn, the maximum number of cycles until the yielding transition is $n_Y = 685$ for the strain amplitude $\gamma_0 = 0.069$. We comment that simulations at smaller strain amplitudes, $\gamma_0 < 0.069$, were not carried out due to the high computational cost.

The similarity of the functional form for potential energy minima shown in Fig. 3 suggests a possibility of rescaling the \hat{x} -coordinate by the number of cycles, n_Y , required for the system to reach the yielding transition at a given strain amplitude. Fig. 4 shows the same potential energy curves as a function of the ratio n/n_Y . Remarkably, the data for different γ_0 nearly

collapse onto a single curve when $n < n_Y$. The master curve is approximately linear in the range $0.2 \lesssim n/n_Y \lesssim 0.8$, followed by a steep increase due to accumulation of plastic events within a narrow region that ultimately leads to flow localization when $n = n_Y$. On the other end, the initial slope of the curve is determined by irreversible rearrangements of group of atoms that settled at relatively shallow energy minima after thermal annealing. In practice, the function $U(n/n_Y)$ can be used to estimate n_Y for a binary glass loaded for a number of cycles ($n < n_Y$) at a strain amplitude in the vicinity of the critical value.

Furthermore, the variation of n_Y versus γ_0 is shown in the inset of Fig. 4. It is readily apparent that the number of cycles until yielding increases significantly when the strain amplitude approaches a critical value from above. Moreover, the MD data are well described by the power-law function, as follows:

$$n_Y = 0.024 \cdot (\gamma_0 - 0.067)^{-1.66}, \quad (3)$$

where the critical strain amplitude is taken to be 0.067. This value was determined previously for a smaller system of 60 000 atoms at $T_{LJ} = 0.01 \varepsilon/k_B$ and $\rho = 1.2 \sigma^{-3}$ [31]. These results imply that the number of cycles to reach the yielding transition might further increase at lower strain amplitudes and possibly diverge in the case of athermal systems [46].

The local plastic events in disordered solids can be accurately identified via the analysis of nonaffine displacements of atoms [47]. As a reminder, the nonaffine measure for displacement of the i -th atom from $\mathbf{r}_i(t)$ to $\mathbf{r}_i(t + \Delta t)$ is defined via the matrix \mathbf{J}_i that transforms positions of its neighboring atoms and minimizes the following expression:

$$D^2(t, \Delta t) = \frac{1}{N_i} \sum_{j=1}^{N_i} \left\{ \mathbf{r}_j(t + \Delta t) - \mathbf{r}_i(t + \Delta t) - \mathbf{J}_i [\mathbf{r}_j(t) - \mathbf{r}_i(t)] \right\}^2, \quad (4)$$

where the summation is performed over N_i atoms that are initially located within 1.5σ from $\mathbf{r}_i(t)$. It should be noted that the plastic rearrangement of neighboring atoms during the time interval Δt typically corresponds to values of the nonaffine measure $D^2(t, \Delta t)$ greater than the cage size, which is about 0.1σ for the KA binary glass at $\rho = 1.2 \sigma^{-3}$ [42].

In Fig. 5 we show the fraction of atoms with relatively large nonaffine displacements during one cycle, $D^2[(n-1)T, T] > 0.04 \sigma^2$, for the strain amplitudes $0.069 \leq \gamma_0 \leq 0.075$. We comment that the nonaffine measure was evaluated only for selected cycles due to excessive computational cost for the large system. It is clearly observed that the shape of n_f is similar

to the dependence of energy minima on the number of cycles shown in Fig. 3. Notice a small peak in n_f during the first cycle due to a number of atoms that become arranged in shallow energy minima upon thermal annealing, and, as a result, these atoms are prone to plastic rearrangement under shear deformation. As expected, the yielding transition is clearly marked by a sharp increase in the fraction n_f , indicating extended plastic flow.

In analogy with the potential energy minima shown in Fig. 4, we replot the same data for n_f as a function of the ratio n/n_Y in Fig. 6. It is evident that fractions $n_f(n/n_Y)$ for different values of the strain amplitude approximately follow a common curve. These results indicate that plastic rearrangements of only about 1% of atoms during the first $n_Y/2$ cycles result in the increase of the potential energy reported in Fig. 4. A shear band forms when $n_f \approx 0.14$ at $n = n_Y$. We also note that both n_f and U increase and level out for $n > n_Y$, which reflects widening of a shear band under cyclic shear. In addition, a closer inspection of the data in the inset to Fig. 6 reveals that, on average, the fraction n_f is slightly larger for cyclic loading at higher strain amplitudes.

The spatial distribution of plastic rearrangements can be visualized by plotting positions of atoms with large nonaffine displacements during one shear cycle, i.e., $\Delta t = T$ in Eq. (4). For example, atomic configurations for selected number of cycles are presented in Fig. 7 for the strain amplitude $\gamma_0 = 0.072$ and in Fig. 8 for $\gamma_0 = 0.069$. It can be seen in Fig. 7 (a) that before yielding, atoms with $D^2(200T, T) > 0.04\sigma^2$ are organized into small clusters that are homogeneously distributed. Upon further loading, the glass yields and a shear band forms along the xy plane during the 218-th cycle, as shown in Fig. 7 (c). During the next 7 cycles, the shear band becomes wider, which is consistent with the increase in n_f and U after yielding reported in Figs. 3–6. Similar trends can be observed in Fig. 8 for cyclic loading at $\gamma_0 = 0.069$, except that the orientation of the shear band is along the yz plane. Also, the sequence of snapshots for the strain amplitude $\gamma_0 = 0.075$ during the first 100 cycles was reported in the previous study [29]. Overall, the visualization of plastic events confirm our earlier conclusions regarding the appearance of small clusters of atoms that rearrange irreversibly after a full cycle, followed by the formation of a shear band at the yielding transition, and its subsequent widening upon continued loading.

IV. CONCLUSIONS

In summary, the effect of oscillatory shear on the damage accumulation and yielding transition was investigated using molecular dynamics simulations. The binary glass was prepared by cooling with a computationally slow rate deep into the glass phase and then subjected to periodic shear deformation with strain amplitudes slightly greater than a critical value. It was found that the number of shear cycles until the yielding transition increases approximately as a power-law function of the difference between the strain amplitude and the critical value. We showed that the fatigue process proceeds via a sequence of irreversible rearrangements of small clusters of atoms until a sudden formation of a shear band at the yielding transition. This behavior is reflected in the gradual increase of the potential energy at the end of each cycle and a steep increase near the yielding point. Furthermore, the potential energy minima for different strain amplitudes closely follow a master curve when plotted versus the normalized number of cycles. The master curve can be used to estimate the fatigue lifetime for a binary glass periodically deformed for only a small number of cycles at a strain amplitude near the critical value.

Acknowledgments

Financial support from the National Science Foundation (CNS-1531923) is gratefully acknowledged. Molecular dynamics simulations were carried out at Wright State University's Computing Facility and the Ohio Supercomputer Center using the LAMMPS code [44].

-
- [1] M. F. Ashby and A. L. Greer, Metallic glasses as structural materials, *Scr. Mater.* **54**, 321 (2006).
 - [2] Z. Sha, W. Lin, L. H. Poh, G. Xing, Z. Liu, T. Wang, and H. Gao, Fatigue of metallic glasses, *Appl. Mech. Rev.* **72**, 050801 (2020).
 - [3] T. Egami, T. Iwashita, and W. Dmowski, Mechanical properties of metallic glasses, *Metals* **3**, 77 (2013).
 - [4] C. J. Gilbert, V. Schroeder, and R. O. Ritchie, Mechanisms for fracture and fatigue-crack propagation in a bulk metallic glass, *Metall. Mater. Trans. A* **30**, 1739 (1999).

- [5] B. C. Menzel and R. H. Dauskardt, Stress-life fatigue behavior of a Zr-based bulk metallic glass, *Acta Mater.* **54**, 935 (2006).
- [6] Y. Kurotani and H. Tanaka, Fatigue fracture mechanism of amorphous materials from a density-based coarse-grained model, *Commun. Mater.* **3**, 67 (2022).
- [7] B. Yang, M. L. Morrison, P. K. Liaw, R. A. Buchanan, G. Wang, C. T. Liu, and M. Denda, Dynamic evolution of nanoscale shear bands in a bulk-metallic glass, *Appl. Phys. Lett.* **86**, 141904 (2005).
- [8] X. D. Wang, R. T. Qu, Z. Q. Liu, and Z. F. Zhang, Shear band propagation and plastic softening of metallic glass under cyclic compression, *J. Alloys Compd.* **695**, 2016 (2017).
- [9] T. C. Hufnagel, C. A. Schuh, and M. L. Falk, Deformation of metallic glasses: Recent developments in theory, simulations, and experiments, *Acta Mater.* **109**, 375 (2016).
- [10] Y. Shi, Size-dependent mechanical responses of metallic glasses, *Int. Mater. Rev.* **64**, 163 (2019).
- [11] F. Spaepen, A microscopic mechanism for steady state inhomogeneous flow in metallic glasses, *Acta Metall.* **25**, 407 (1977).
- [12] A. S. Argon, Plastic deformation in metallic glasses, *Acta Metall.* **27**, 47 (1979).
- [13] F. Kun, M. H. Costa, R. N. Costa Filho, J. S. Andrade Jr, J. B. Soares, S. Zapperi, and H. J. Herrmann, Fatigue failure of disordered materials, *J. Stat. Mech.* P02003 (2007).
- [14] J. O. Cochran, G. L. Callaghan, and S. M. Fielding, Slow fatigue and highly delayed yielding via shear banding in oscillatory shear (2022). arXiv:2211.11677
- [15] N. V. Priezjev, Heterogeneous relaxation dynamics in amorphous materials under cyclic loading, *Phys. Rev. E* **87**, 052302 (2013).
- [16] I. Regev, T. Lookman, and C. Reichhardt, Onset of irreversibility and chaos in amorphous solids under periodic shear, *Phys. Rev. E* **88**, 062401 (2013).
- [17] D. Fiocco, G. Foffi, and S. Sastry, Oscillatory athermal quasistatic deformation of a model glass, *Phys. Rev. E* **88**, 020301(R) (2013).
- [18] I. Regev, J. Weber, C. Reichhardt, K. A. Dahmen, and T. Lookman, Reversibility and criticality in amorphous solids, *Nat. Commun.* **6**, 8805 (2015).
- [19] Z. D. Sha, S. X. Qu, Z. S. Liu, T. J. Wang, and H. Gao, Cyclic deformation in metallic glasses, *Nano Lett.* **15**, 7010 (2015).
- [20] N. V. Priezjev, Reversible plastic events during oscillatory deformation of amorphous solids,

- Phys. Rev. E **93**, 013001 (2016).
- [21] T. Kawasaki and L. Berthier, Macroscopic yielding in jammed solids is accompanied by a non-equilibrium first-order transition in particle trajectories, Phys. Rev. E **94**, 022615 (2016).
- [22] N. V. Priezjev, Nonaffine rearrangements of atoms in deformed and quiescent binary glasses, Phys. Rev. E **94**, 023004 (2016).
- [23] P. Leishangthem, A. D. S. Parmar, and S. Sastry, The yielding transition in amorphous solids under oscillatory shear deformation, Nat. Commun. **8**, 14653 (2017).
- [24] N. V. Priezjev, Collective nonaffine displacements in amorphous materials during large-amplitude oscillatory shear, Phys. Rev. E **95**, 023002 (2017).
- [25] N. V. Priezjev, Molecular dynamics simulations of the mechanical annealing process in metallic glasses: Effects of strain amplitude and temperature, J. Non-Cryst. Solids **479**, 42 (2018).
- [26] N. V. Priezjev, The yielding transition in periodically sheared binary glasses at finite temperature, Comput. Mater. Sci. **150**, 162 (2018).
- [27] A. D. S. Parmar, S. Kumar, and S. Sastry, Strain localization above the yielding point in cyclically deformed glasses, Phys. Rev. X **9**, 021018 (2019).
- [28] N. V. Priezjev, Accelerated relaxation in disordered solids under cyclic loading with alternating shear orientation, J. Non-Cryst. Solids **525**, 119683 (2019).
- [29] N. V. Priezjev, Shear band formation in amorphous materials under oscillatory shear deformation, Metals **10**, 300 (2020).
- [30] W. T. Yeh, M. Ozawa, K. Miyazaki, T. Kawasaki, and L. Berthier, Glass stability changes the nature of yielding under oscillatory shear, Phys. Rev. Lett. **124**, 225502 (2020).
- [31] N. V. Priezjev, Alternating shear orientation during cyclic loading facilitates yielding in amorphous materials, J. Mater. Eng. Perform. **29**, 7328 (2020).
- [32] N. V. Priezjev, A delayed yielding transition in mechanically annealed binary glasses at finite temperature, J. Non-Cryst. Solids **548**, 120324 (2020).
- [33] H. Bhaumik, G. Foffi, and S. Sastry, The role of annealing in determining the yielding behavior of glasses under cyclic shear deformation, PNAS **118**, 2100227118 (2021).
- [34] N. V. Priezjev, Accessing a broader range of energy states in metallic glasses by variable-amplitude oscillatory shear, J. Non-Cryst. Solids **560**, 120746 (2021).
- [35] N. V. Priezjev, Yielding transition in stable glasses periodically deformed at finite temperature, Comput. Mater. Sci. **200**, 110831 (2021).

- [36] S. Cui, H. Liu, and H. Peng, Anisotropic correlations of plasticity on the yielding of metallic glasses, *Phys. Rev. E* **106**, 014607 (2022).
- [37] B. P. Bhowmik, H. G. E. Hentchel, and I. Procaccia, Fatigue and collapse of cyclically bent strip of amorphous solid, *EPL* **137**, 46002 (2022).
- [38] N. V. Priezjev, Mechanical annealing and yielding transition in cyclically sheared binary glasses, *J. Non-Cryst. Solids* **590**, 121697 (2022).
- [39] A. Elgailani, D. Vandembroucq, and C. E. Maloney, Anomalous softness in amorphous matter in the reversible plastic regime (2022). [arXiv:2212.10472](https://arxiv.org/abs/2212.10472)
- [40] B. Shang, N. Jakse, P. Guan, W. Wang, and J.-L. Barrat, Influence of oscillatory shear on nucleation in metallic glasses: A molecular dynamics study, *Acta Mater.* **246**, 118668 (2023).
- [41] C. Reichhardt, I. Regev, K. Dahmen, S. Okuma, and C. J. O. Reichhardt, Perspective on reversible to irreversible transitions in periodic driven many body systems and future directions for classical and quantum systems (2022). [arXiv:2211.03775](https://arxiv.org/abs/2211.03775)
- [42] W. Kob and H. C. Andersen, Testing mode-coupling theory for a supercooled binary Lennard-Jones mixture: The van Hove correlation function, *Phys. Rev. E* **51**, 4626 (1995).
- [43] T. A. Weber and F. H. Stillinger, Local order and structural transitions in amorphous metal-metalloid alloys, *Phys. Rev. B* **31**, 1954 (1985).
- [44] S. J. Plimpton, Fast parallel algorithms for short-range molecular dynamics, *J. Comp. Phys.* **117**, 1 (1995).
- [45] M. P. Allen and D. J. Tildesley, *Computer Simulation of Liquids* (Clarendon, Oxford, 1987).
- [46] J. T. Parley, S. Sastry, and P. Sollich, Mean-field theory of yielding under oscillatory shear, *Phys. Rev. Lett.* **128**, 198001 (2022).
- [47] M. L. Falk and J. S. Langer, Dynamics of viscoplastic deformation in amorphous solids, *Phys. Rev. E* **57**, 7192 (1998).

Figures

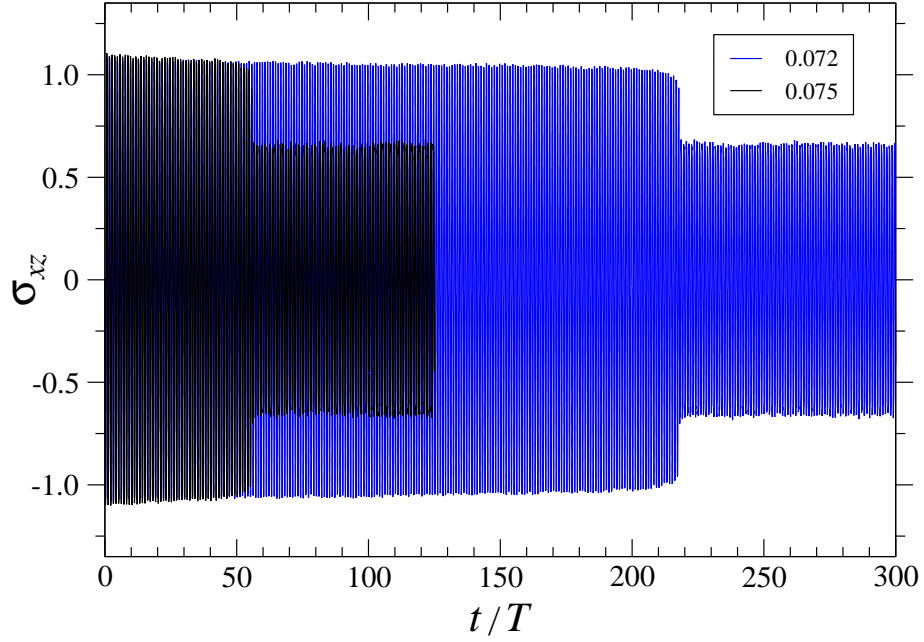


FIG. 1: (Color online) The shear stress, σ_{xz} (in units $\varepsilon\sigma^{-3}$), versus cycle number for strain amplitudes $\gamma_0 = 0.072$ (blue curve) and $\gamma_0 = 0.075$ (black curve). The period of oscillation is $T = 5000\tau$.

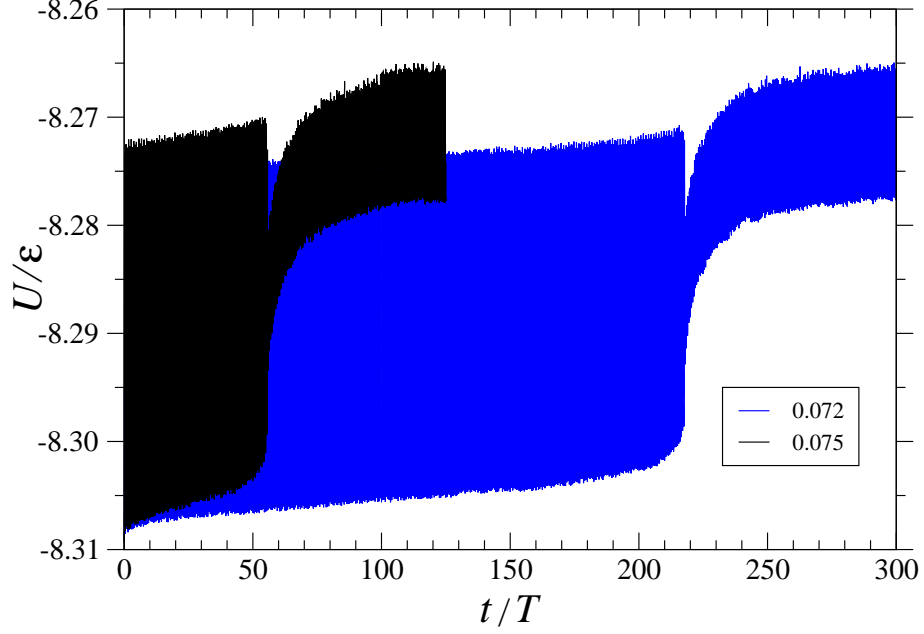


FIG. 2: (Color online) The potential energy per atom, U/ε , as a function of time for strain amplitudes $\gamma_0 = 0.072$ (blue curve) and $\gamma_0 = 0.075$ (black curve). The period of oscillation is $T = 5000\tau$. The binary glass was initially prepared by cooling from $T_{LJ} = 1.0\varepsilon/k_B$ to $0.01\varepsilon/k_B$ with the rate of $10^{-5}\varepsilon/k_B\tau$ at $\rho = 1.2\sigma^{-3}$.

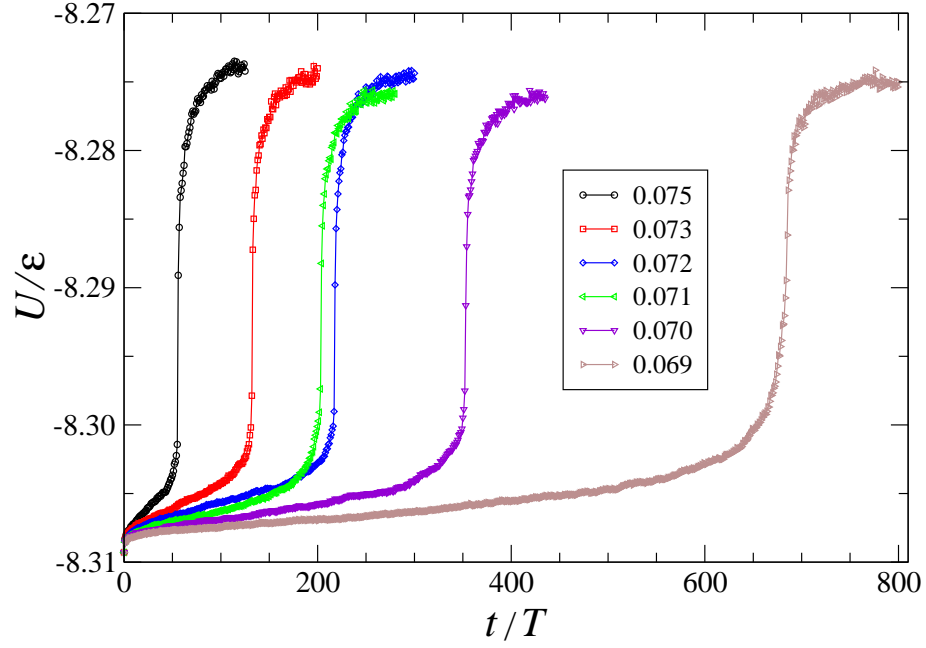


FIG. 3: (Color online) The potential energy minima at the end of each shear cycle for strain amplitudes $\gamma_0 = 0.069, 0.070, 0.071, 0.072, 0.073,$ and 0.075 (from right to left). The oscillation period is $T = 5000 \tau$.

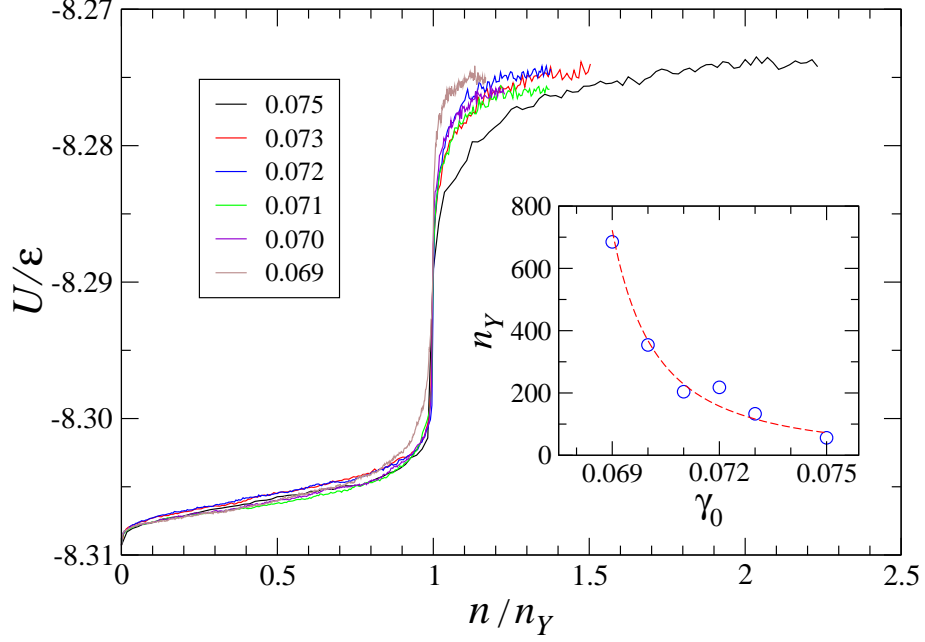


FIG. 4: (Color online) The potential energy minima as a function of the ratio, n/n_Y , where $n = t/T$ is the cycle number and n_Y is the number of cycles to yield at a given strain amplitude. The same data as in Fig. 3. The symbols are omitted for clarity. The inset shows n_Y versus the strain amplitude γ_0 . The dashed red curve is the best fit to the data given by Eq. (3).

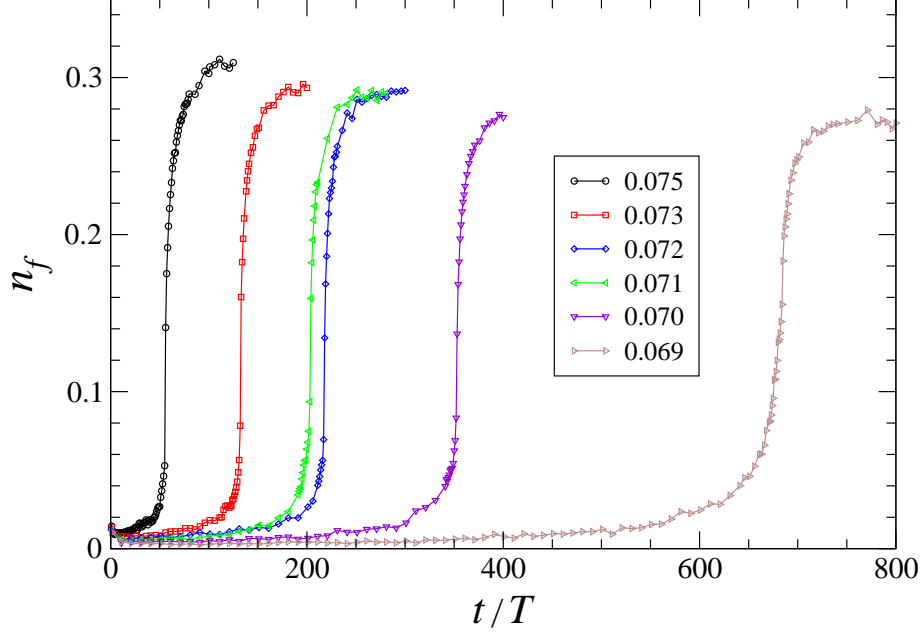


FIG. 5: (Color online) The fraction of atoms with large nonaffine displacements, $D^2[(n-1)T, T] > 0.04\sigma^2$, as a function of the cycle number for the indicated values of the strain amplitude γ_0 . Here, $n = t/T$ is the cycle number, and $T = 5000\tau$ is the oscillation period.

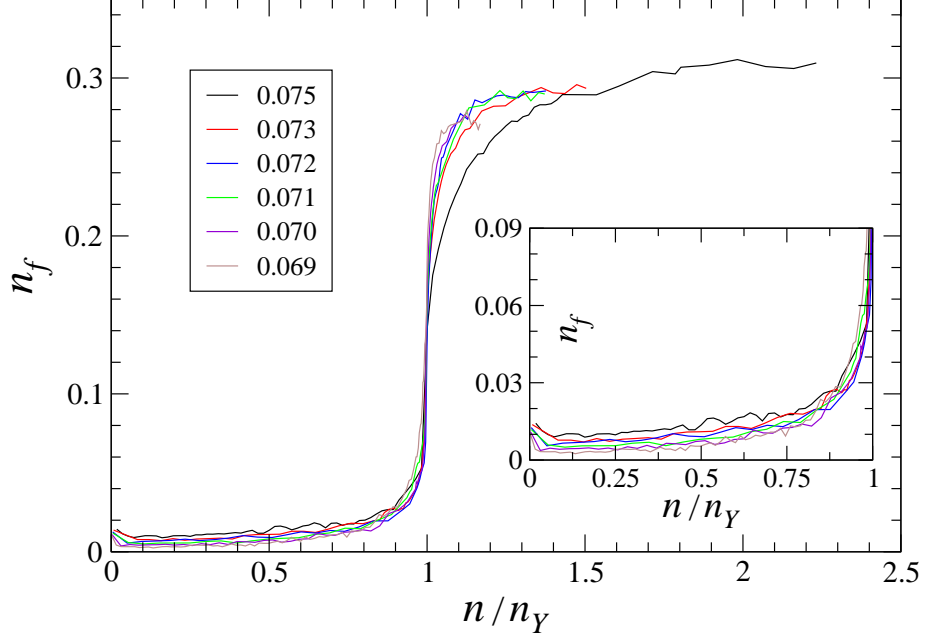


FIG. 6: (Color online) The fraction of atoms with $D^2[(n-1)T, T] > 0.04\sigma^2$ versus the ratio n/n_Y , where n is the cycle number and n_Y is the number of cycles until yielding. The values of n_Y are reported in Fig. 4. The symbols are not shown for clarity. The inset shows an enlarged view of the same data for $n/n_Y \leq 1$.

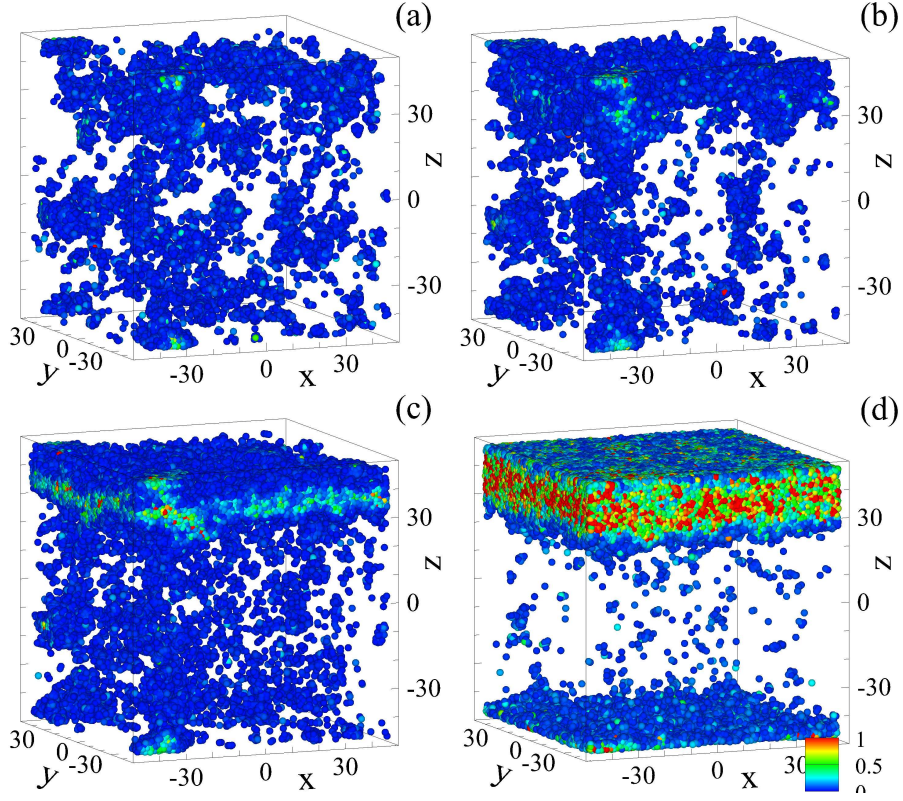


FIG. 7: (Color online) The atomic configurations of the binary glass loaded at the strain amplitude $\gamma_0 = 0.072$. The nonaffine displacements are shown for atoms with the nonaffine measure (a) $D^2(200T, T) > 0.04\sigma^2$, (b) $D^2(216T, T) > 0.04\sigma^2$, (c) $D^2(217T, T) > 0.04\sigma^2$, and (d) $D^2(224T, T) > 0.04\sigma^2$. The legend color denotes the magnitude of D^2 . The atoms are not drawn to scale.

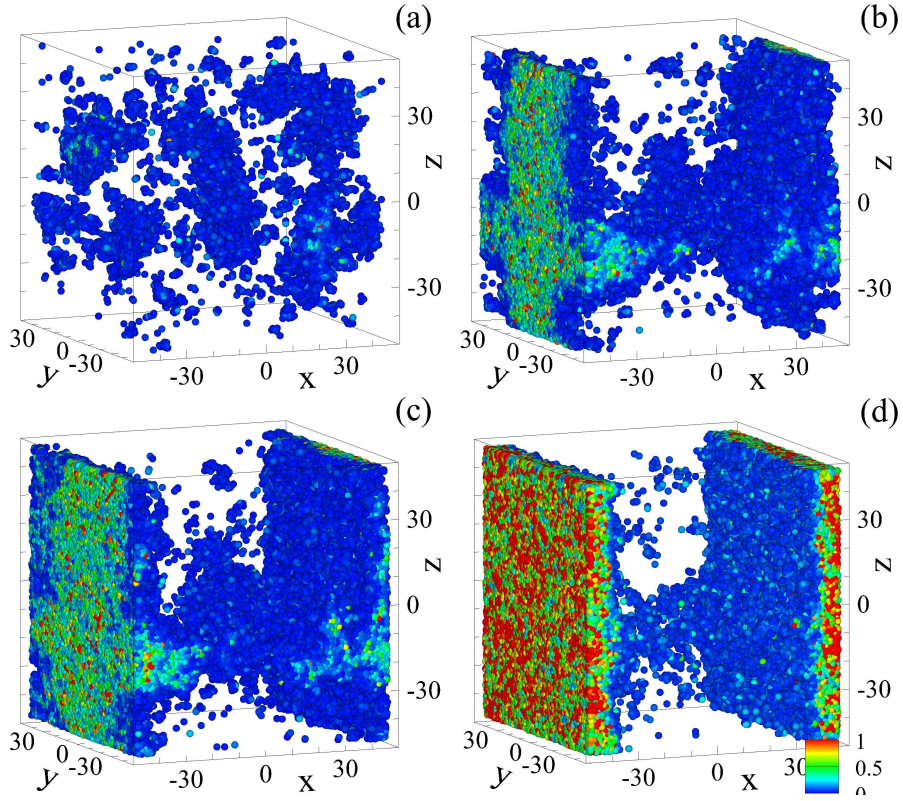


FIG. 8: (Color online) Snapshots of the well-annealed glass subjected to cyclic shear with the strain amplitude $\gamma_0 = 0.069$. The nonaffine measure is (a) $D^2(600T, T) > 0.04\sigma^2$, (b) $D^2(683T, T) > 0.04\sigma^2$, (c) $D^2(684T, T) > 0.04\sigma^2$, and (d) $D^2(689T, T) > 0.04\sigma^2$. The colorcode indicates values of D^2 .